Langmuir

ARTICLE

pubs.acs.org/Langmuir

# Cellular Compatibility of Biomineralized ZnO Nanoparticles Based on Prokaryotic and Eukaryotic Systems

Danhong Yan,[†] Guangfu Yin,[‡] Zhongbing Huang,[*,‡] Liang Li,[*,†] Xiaoming Liao,[‡] Xianchun Chen,[‡] Yadong Yao,[‡] and Baoqing Hao[*,§]

[†]Institute of Biomedical Engineering, School of Preclinical and Forensic Medicine, Sichuan University, Chengdu, 610041, P. R. China

[‡]College of Materials Sciences and Engineering, Sichuan University, Chengdu, 610065, P. R. China

[§]College of Life Science & Technology, Southwest University for Nationalities, Chengdu, 610041, P. R. China

**ABSTRACT:** Zinc oxide nanoparticles (NPs) with the size of ~100 nm were prepared via a facile biomineralization process in the template of silk fibroin (SF) peptide at room temperature. These ZnO NPs have shown the remarkable behavior of low toxicity to Gram-positive bacteria (*Staphylococcus aureus*, *Staphylococcus agalactiae*), Gram-negative bacteria (*Escherichia coli*), and eukaryotic cells (mouse L929 fibroblasts). Bacteriological testing indicated that ZnO NPs presented a 50% inhibitory effect on *Streptococcus agalactiae* at the concentrations of >100 mM, whereas at the same concentrations, the growth of *Staphylococcus aureus* and *Escherichia coli* were hardly inhibited. On the other hand, a remarkable proliferation of *Staphylococcus aureus* or *Escherichia coli* was observed at the concentrations of ZnO NPs <50 mM. Moreover, the cytotoxicity test demonstrated that ZnO NPs mineralized with SF peptide possessed a low toxicity to mouse L929 fibroblasts. The SF peptide coated on the surface of ZnO NPs permitted greater adhesion and consequently greater proliferation of mouse L929 fibroblasts. Besides, from TEM micrographs of the cell ultrastructure, endocytosis of NPs into the cytoplasm can be detected and the ultrastructure of the cell underwent few changes. The cell membrane retained integrity, euchromatin dispersed homogenously inside the cytoplasm, the mitochondrial architecture remained intact, and no intracellular vacuoles were observed. High-resolution transmission electron microscopy images and selected area electron diffraction patterns of ultrathin cell sections indicated that the crystal structure of NPs was not damaged by the organelle or cytoplasm. All these observations indicated that ZnO NPs mineralized with the SF peptide possess good cytocompatibility.

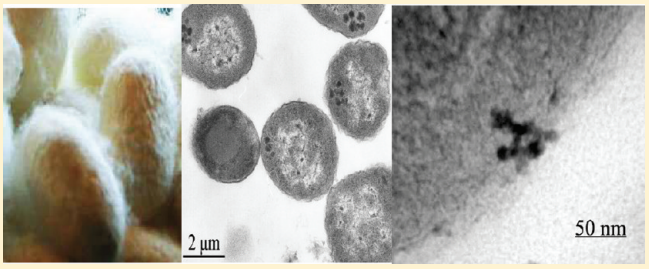


## 1. INTRODUCTION

Since the manufacture and application of metal oxide nanoparticles (NPs) have been increasing, human beings are more likely to be exposed occupationally or via consumer products and the environment. NPs, due to the high surface-to-volume ratio, may interact with biological molecules and tissues by more efficient approaches and result in grave toxicity.[1−4] So far, numerous studies of nanotoxicity *in vivo*/*vitro* have been performed to assess the biological effects of various kinds of manufactured NPs. Some studies revealed that magnetic iron oxide NPs could localize to the membrane of human dermal fibroblasts and cause cell death.[5−7] Sunlight-illuminated nanosized $TiO_2$ could catalyze DNA damage both *in vitro* and in human cells[8] and sometimes could be used to fight anthrax or even cancer.[9]

ZnO NPs are believed to be nontoxic, biosafe, and biocompatible[10] and have achievable applications in daily life, such as drug carriers, cosmetics additives, and medical materials fillings.[11,12] However, some experts have observed its toxicological effects on target microorganisms.[13−15] Nano-ZnO was found to be capable of reaching the alveoli and inducing pulmonary inflammation and metal fume fever in rats.[16] Acute exposure of ZnO NPs on human aortic endothelial cells could significantly regulate mRNA levels of inflammatory Interleukin-8.[17] Therefore, the study of the nontoxic and excellent biocompatible ZnO nanomaterials is attracting growing interest.

Müller et al. confirmed that the release of $Zn^{2+}$ may be a key factor in the cytotoxicity of ZnO NPs.[18] The surface chemistry of NPs is one of the critical factors determining cellular responses *in vitro*.[19] Hoshino et al. reported that quantum dots coated with carboxyl groups were less toxic than those with an anime surface coating.[20] Müller et al. reported that the cytotoxicity of iron oxide NPs could be reduced by a dextran surface layer.[21] Cao et al. found that the coating of biocompatible carbon remarkably reduced the cytotoxicity of ZnO nanorods.[22] These observations indicated that the toxicity of ZnO NPs could be regulated by changing their surface chemistry. The surface modification of NPs (surface covered with functional groups or biomacromolecules) could specify the biological behavior of the whole NPs. However, the reports about the coated ZnO NPs are rather limited.[22−24]

**Received:** March 3, 2011
**Revised:** September 9, 2011
**Published:** September 21, 2011

In this study, we demonstrated a mild room-temperature aqueous solution mineralization process to prepare ZnO NPs coated with silk fibrion (SF). Meanwhile, the toxicological impacts on bacteria (*Staphylococcus aureus*, *Escherichia coli*, and *Streptococcus agalactiae*) and eukaryotic cells (mouse L929 fibroblasts) were assessed. Furthermore, high-resolution transmission electron microscopy (HRTEM) and selected area electron diffraction (SAED) were used to investigate the interaction between the ultramicrostructure of the cells and the crystal structure of ZnO NPs. The surface chemistry influence on the physical and chemical properties of the ZnO NPs and the associated biological effects were discussed.

## 2. MATERIALS AND METHODS

**2.1. Materials.** *Bombyx mori* silk fiber was purchased commercially. Luria−Bertani (LB) medium used for growing and maintaining bacterial cultures were purchased from Sigma-Aldrich (UK). *Staphylococcus aureus*, *Escherichia coli*, and *Streptococcus agalactiae* were kindly provided by Cell-Biology Laboratory of Southwest University for Nationalities. L929 mouse fibroblasts were gifted by College of Life and Science, Sichuan University. Other chemicals used in this study were all analytical grade purchased from Chengdu Chemical Co. Ltd. (China).

**2.2. Biomineralization of ZnO NPs.** *B. mori* silk fiber was boiled in 0.3% $Na_2CO_3$ solution for 30 min to degum the glue-like sericin coating, then dried and hydrolyzed in 6 M HCl at 80 °C for 12 h. The SF hydrolysate solution was adjusted to pH 7 and dialyzed with distilled water at 4 °C for about 24 h. 0.1 M zinc nitrate solution was mixed with the same volume of 0.2 M sodium hydrate. The $Zn(OH)_2$ produced was rinsed several times with distilled water, and the final concentration of $Zn(OH)_2$ was adjusted to 0.1 M. Two milliliter solution of SF peptide (0.1 mg/mL) was added to 40 mL $Zn(OH)_2$ solution, and the solution was incubated at room temperature for 6 h. After centrifugation and washing with distilled water and alcohol three times, respectively, ZnO particles were dried at room temperature.

**2.3. Characterization of ZnO NPs.** The morphology of the ZnO particles was characterized using scanning electron microscopy (SEM, JEOL-5900LV, 20 kV). The shapes and crystalline structures of synthesized crystals were studied by transmission electron microscopy (TEM, JEOL-200, 160 kV, Philips TECNAI 20 high resolution (HR) TEM at 400 kV) and accompanying selected area electron diffraction (SAED) and scanning electron microscopy (SEM, JEOL-5900LV, 20 kV). X-ray diffraction (XRD) patterns were recorded on a Philips X′Pert MDP diffractometer with Cu K$\alpha$ radiation. Fourier transform infrared (FT-IR) spectra were recorded by an IRPrestige-21 spectrometer.

**2.4. Cytotoxicity of ZnO NPs on Prokaryotic Cells.** These three strains of *Escherichia coli*, *Staphylococcus aureus*, and *Streptococcus agalactiae* were cultivated aerobically in a Luria−Bertani (LB) medium containing 5 g/L of yeast extract, 10 g/L of tryptone, and 10 g/L of NaCl at 37 °C and pH 7.4 for 18−24 h until the cell count reached a minimum of $10^8$ CFU/mL. The inoculated cells were estimated to about 200 CFU per plate, and all results were compared to a control without ZnO particles. Bacteria together with mineralized ZnO particles cultured on solid agar plates were then incubated at 37 °C overnight, and the colony counts were taken the next day. All experiments were conducted in triplicate for each strain.

**2.5. Cytotoxicity of ZnO NPs on Eukaryotic Cells.** A mouse fibroblast cell line (L929) was used to evaluate the cytotoxicity and proliferative effect of biomineralied ZnO NPs. The cells were cultured in RPMI medium 1640 (Gibco) supplemented with 10% fetal bovine serum (Gibco), 1 mM L-glutamina, penicillin (20 000 U/mL), and streptomycin (20 000 $\mu$g/mL), under a $CO_2$ (5%) atmosphere at 37 °C. The *in vitro* cytotoxicity of ZnO NPs upon L929 cells was determined by the 3-(4,5-dimethylthiazol-2-yl)-2,5-diphenyltetrazolium bromide (MTT) assay. In a classic experiment, 150 $\mu$L cell suspensions were plated into 96-well plates (BD Biosciences) at an initial density of approximately $2 \times 10^4$ cells/well. When the cells reached confluence, 50 $\mu$L ZnO suspensions of varying concentrations were added and the plates were cultured at 37 °C. The cells without adding any particles were used as the control and the wells without cultured cells but with different density of particles were tested as the blank contrast. Each concentration was set for six parallel samples during the process. At the end of the designed incubation time, 20 $\mu$L 5 mg/mL MTT-PBS solution was added to each well and the plates were incubated for another 4 h. Finally, the solution was removed and 150 $\mu$L dimethyl sulfoxdie (DMSO) was added in each well to dissolve the formed violet substance. Plates were read using Beckman DU 640 UV−visible spectrophotometer at an absorbance at 570 nm.

**2.6. Cell Ultrathin Structure Observation.** Cells exposed to 0.1 mg/mL ZnO NPs for designated times were washed three times with PBS and fixed with Karnovsky's EM fixative (2.5% glutaraldehyde and 2% paraformaldehyde in 80 mM phosphate buffer, pH 7.3−7.4). Secondary fixation was done in 1% osmium tetroxide with 1.5% potassium ferrocyanide in double distilled $H_2O$ for 1 h at 4 °C. Dehydration was performed through ascending concentrations of ethanol with three changes at 100%. Pure Epon-Araldite resin that did not contain methyl anhydride was added and infiltrated overnight at room temperature. All resin was removed the next day, and fresh resin was added to the appropriate depth. The sample was polymerized for 18 h. Ultrathin sections of cells of interest were cut *en face* (parallel to the surface on which the cells were grown) using a Leica Ultracut UCT ultramicrotome (MT-X; RMCInc., Tucson, AZ) and then stained with uranyl acetate and lead citrate before viewing using a transmission electron microscopy (TEM, JEOL-200, 160 kV).

**2.7. Analysis of ZnO NP Uptake by SEM/EDX.** L929 were grown on 10 mm coverslips and incubated with 0.1 mg/mL ZnO NPs for 24 h. Then, the coverslips were quickly dipped twice in ice-cold distilled water, quench−frozen in propane cooled in liquid nitrogen, freeze−dried. In order to minimize interference induced by the other substance during the preparation. Neither gold nor carbon coating was applied to the coverslips. The SEM images and an accompanying EDX were performed to analyze the composition of the samples.

**2.8. Statistics.** Data are expressed as means ± standard deviation. Statistical analysis was performed using the *Statistical Package for the Social Sciences* (SPSS) v 13.0 software. Statistical comparisons were made by analysis of variance (ANOVA). Scheffé and Games-Howell tests were used for post hoc evaluations of differences between groups. In all statistical evaluations, $p < 0.05$ was considered statistically significant.

## 3. RESULTS AND DISCUSSION

Figure 1a showed the XRD pattern of biomineralized particles. The result could be readily indexed to a pure zincite of ZnO with lattice constants $a$ = 3.250 Å, $b$ = 3.250 Å, and $c$ = 5.207 Å (JCPDS 36−1451). No characteristic peaks from other phases were observed, indicating that $Zn(OH)_2$ have been completely hydrolyzed to ZnO capped with the SF peptide assemblies. In general, there are two factors that may influence the size and the shape of ZnO NPs in the process of biomineralization: (i) the nature of the molecular template added during ZnO formation and (ii) the biomineralization time.[25] Figure 1b illustrated the IR absorption spectrum of mineralized ZnO particles. A peak at 3428 $cm^{-1}$ was the stretching vibration of the H−O bond. Two peaks at 1624 and 1388 $cm^{-1}$ were assigned to the vibration of amide I and amide II, respectively, and the peak of phenyl group from phenylalanine centered at ∼887 $cm^{-1}$, suggesting that SF peptide has assembled with ZnO particles. A peak at ∼478 $cm^{-1}$ was the stretching vibration of the Zn−O bond in ZnO particles. The SEM image in Figure 1c showed that the size of spherical

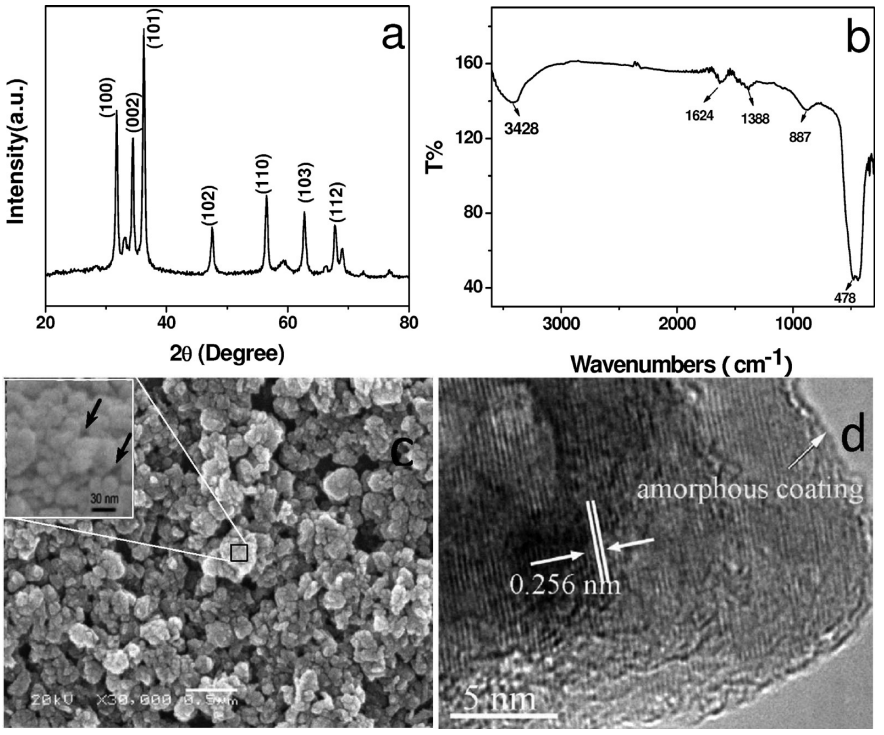


**Figure 1.** (a) XRD pattern, (b) FT-IR absorption spectrum, (c) SEM image, and (d) HRTEM image of ZnO NPs biomineralized after 6 h.

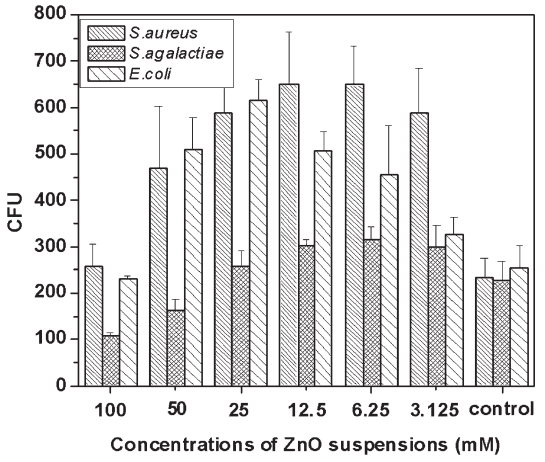


**Figure 2.** Means and standard errors of CFU per plate of *S. aureus*, *S. agalactiae* ,and *E. coli* incubated for 24 h in LB media in the presence of different concentrations of ZnO suspensions; $n = 3$.

NPs was about 100 nm. Most of the particles were aggregated by ultrafine primary particles with a size of 20−30 nm and an interstice of 5−8 nm between particles (pointed out by arrows in the inset), indicating that the mineralized NPs had hierarchical structures. The obvious porous feature indicated that the nanometer-sized grains were uniformly distributed and interconnected to form a "netlike" structure, which was consistent with our previous result.[26] The measured distance between parallel lattice planes was 0.256 nm (Figure 1d). Although there were crystalline dislocations and defects, a high-quality crystalline structure of ZnO was prepared by the biomineralization process under room temperature. In addition, a thin amorphous coating layer (marked with a white arrow in Figure 1d) was observed on the surface of a mineralized NP, indicating that the SF peptide was probably incorporated into ZnO NPs during the biomineralization, which was consistent with the result of FT-IR.

The agar plates test is one of the standard *in vitro* susceptibility tests recommended by the National Committee for Clinical Laboratory Standards (NCCLS).[27,28] Figure 2 presented the bacterial colonies of *S. aureus*, *S. agalactiae*, and *E. coli* cultured with different concentrations of ZnO NPs. The result showed that ZnO NPs had 50% inhibitory effect on *S. agalactiae* at the concentrations of >100 mM. In contrast, the same concentration of ZnO NPs caused no significant decrease in viability of *S. aureus* or *E. coli*. At the concentration of 50 mM, ZnO NPs induced a remarkable promotion of *S. aureus* and *E. coli*, while a slight inhibitory action still existed on *S. agalactia*. And, ≤25 mM of ZnO NPs significantly promoted bacterial growths of all groups. These observations partly suggested that the mineralized ZnO NPs possessed favorable cytocompatibility. The relatively low toxicity of NPs to *S. aureus* or *E. coli* was probably due to the relatively high Zn-ion tolerance.

In order to quantify the toxicity of ZnO NPs to L929 fibroblast cells, MTT assay was performed to determine the survival rate of cells in the presence of varying concentrations of ZnO NPs. After 24 h, a high dose of ZnO (2.5 mg/mL and 0.5 mg/mL) showed a significant effect ($p < 0.05$) to restrain cell proliferation, while at lower concentrations (0.1−0.004 mg/mL), all of the experimental groups showed high resistance to the cytotoxicity of ZnO NPs, and the cell viabilities of those groups were close to 100%. After 48 h, 0.004 mg/mL ZnO NPs displayed a significant effect to advance the proliferation of L929 cells. After 3 d, 0.02 and 0.004 mg/mL ZnO NPs had significant effects to promote the proliferation of cells. It was reported that 20 ug/mL ZnO NPs were capable of producing significant cytotoxicity to A549 cells.[29] Rod-shaped ZnO NPs with lengths of 100−200 nm and diameters of 20−70 nm were toxic to human aortic endothelial

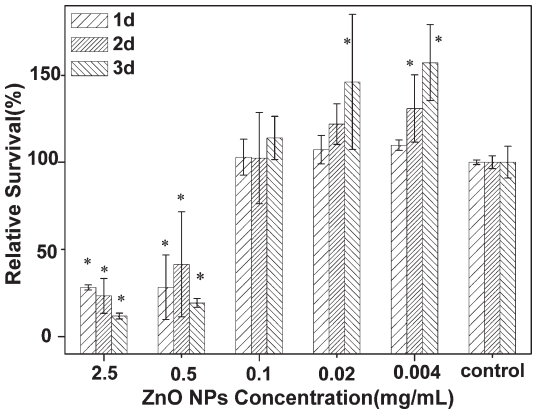


**Figure 3.** Cell viability of L929 cells incubated with different concentrations of mineralized ZnO NPs at 37 °C for 1−3 days. Error bars indicate standard deviation. * represents significant difference. Cell viability was determined by the MTT assay and expressed as a percentage of the control wells (cells without NPs treatment).

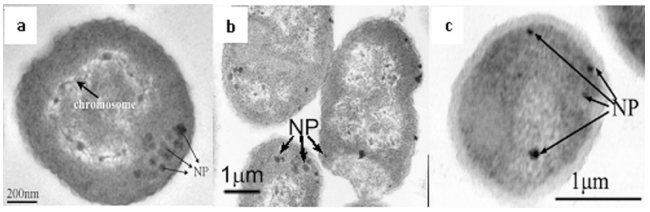


**Figure 4.** TEM images of ultrathin section of (a) *S. agalactiae*, (b) *S. aureus*, and (c) *E. coli* exposed with 0.1 mg/mL ZnO NPs for 18 h, where NP = ZnO NPs. Endocytosis of NPs into the cytoplasm was detected, the cell membrane retained integrity, and no intracellular vacuole was observed.

cells at 10 and 50 $\mu$g/mL.[17] However, in our work, ZnO NPs with the concentration of 20 $\mu$g/mL could significantly promote proliferation instead of producing cytotoxicity. We suggested that the SF peptide coated on the surface of NPs played an important role in the cellular compatibility.

TEM micrographs of cell ultrastructure allowed direct visualization of morphology changes of cells after contacting with ZnO NPs. *S. agalactiae* and *S. aureus* are two kinds of Gram-positive cocci. Figure 4a,b showed that ZnO NPs (marked by black arrows) could cross the cell membrane and internalize inside the cell. Furthermore, the cell membrane remained intact, euchromatin dispersed homogenously inside the cytoplasm, and none of the intracellular vacuole was observed. *E. coli* is a moderately sized Gram-negative bacillus that presents a tubular form. Figure 4 displayed the cross section of a typical *E. coli*, and the organized triple membrane of the cell was clearly observed. The cell membrane of *E. coli* was intact and the intracellular content did not leak out. Cellular endocytosis of ZnO NPs could also be observed and cell walls retained integrity. All these observations indicated that the ZnO NPs had low cytotoxicity on both Gram-positive and -negative bacteria, which were consistent with the results of the solid plates test.

Figure 5b−d showed TEM micrographs of L929 fibroblast cells cultured in RPMI 1640 medium with 0.1 mg/mL ZnO NPs for 1−3 days. Compared with the TEM image of L929 cultured in ZnO-free medium (Figure 5a), inconspicuous damage in the morphology of the experimental cells was detected (Figure 5b−d).

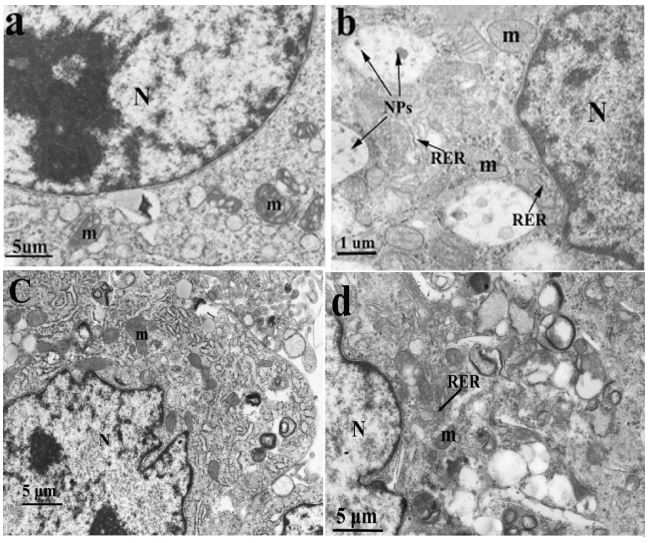


**Figure 5.** TEM images of L929 cell cultured in RPMI medium 1640 (a) without ZnO and with 0.1 mg/mL ZnO for (b) 24 h, (c) 48 h, and (d) 72 h, respectively, where N = nucleus, m = mitochondria, RER = rough endoplasmic reticulum, and NPs = ZnO NPs. Endocytosis of NPs into the cytoplasm was detected and few intracellular vacuoles were observed. The mitochondria, ribosomes, and rough endoplasmic reticulum were not destroyed.

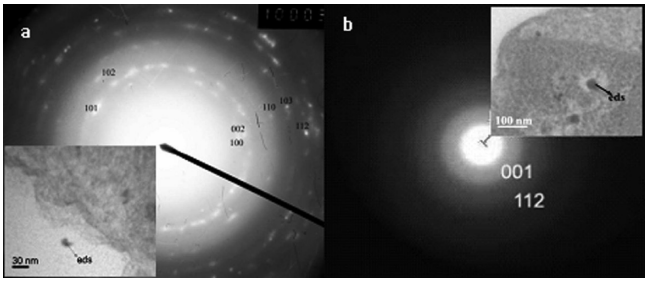


**Figure 6.** SAED patterns ZnO NPs (a,b) outside and (c,d) inside *S. aureus* cells. Insets illustrated the corresponding locations of NPs.

It was seen that L929 cell had an irregular nucleus, a homogenously dispersed euchromatin, and a sunken nuclear membrane. In the cytoplasm, the mitochondria, ribosomes, and rough endoplasmic reticulum were all clearly observed. Cellular endocytosis of ZnO NPs could be identified and the ultrastructure of the cell underwent few changes. These observations showed that the ZnO NPs had no cytotoxicity effect upon L929 cells at a concentration of 0.1 mg/mL, which was consistent with the result of the MTT assay. In addition, ZnO NPs internalized inside the cytoplasm were eliminated along with the increase of incubation time.

In order to confirm whether the NPs detected in the ultrathin cell section were ZnO NPs, HRTEM observation and SAED analysis were carried out. Figure 6a,b showed SAED patterns of mineralized NPs outside and inside *S. aureus*. The electron diffraction pattern of an isolated species, recorded from one NP, revealed that NPs in the cytoplasm could retain the zincite structure of ZnO crystal. Due to the organic supporting carbon film, which was used for the preparation of ultrathin cell sections, the dispersion rings of mineralized NPs inside cells were not clear, but (112) and (001) planes could be easily distinguished in

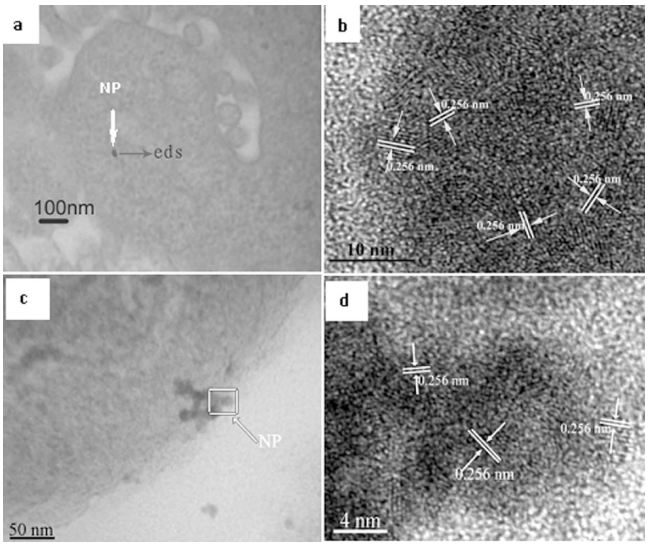


**Figure 7.** HRTEM images of ZnO NPs (b,d) in the corresponding regions of (a) L929 and (c) *S. aureus* cells. Endocytosis of ZnO NPs into the cytoplasm was detected (a,c), and the distance between two parallel lattice planes was 0.256 nm (b,d).

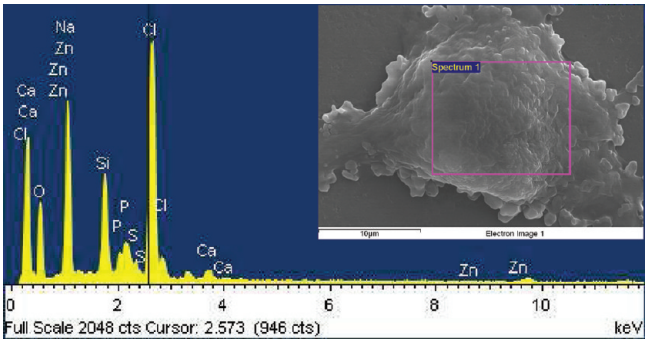


**Figure 8.** SEM and EDX analysis of ZnO uptake in L929. Cells were incubated in culture medium with 0.1 mg/mL ZnO NPs. The image inset in the right shows cells in detail.

Figure 6b. These results indicated that the crystal structure of NPs did not change inside the cell.

Figure 7b,d shows the magnifying HRTEM images of ZnO NPs detected in L929 cell (Figure 7a) and *S. aureus* (Figure 7c). The measured distance (0.256 nm) between two parallel lattice planes was [001] crystal direction, indicating that the ZnO crystal structure could be retained in cells, which was coincident with the lattice plane of Figure 1d. The size of ZnO NPs was ~20 nm, which was much smaller than that of original mineralized NPs, but the size of NPs was much closer to the data (~17.4 nm) calculated through the Sheerer formula or the primary particles (~20 nm, inset of Figure 1c). It was apparent that, after encytosis of ZnO NPs inside the cell, the amorphous components (including SF peptide coating layers and crystal defects) in ZnO NPs might be "eaten off" by cytoplasm. In HRTEM results, additionally, the crystal structures of mineralized NPs were not clearly visible as the groups before cell culture. We supposed that, while in contact with NPs cellular endocytosis occurred, the cell sap permeated into the interstice of the NPs, damaging the amorphous structure and inducing the dispersion of the primary particles.

It is clear from HRTEM imaging that some ZnO dissolution had taken place during TEM sample processing. We therefore also used SEM and energy-dispersive X-ray spectrometry (EDX) analysis (Figure 8) to study ZnO NPs uptake in L929. The EDX spectrum clearly showed the presence of zinc. Zinc with about 0.38% in weight was found in the cells.

It should be stressed that metal-containing NPs may cause additional toxic effects via other mechanisms except inducement by solubilized heavy metals. Several nanomaterials including quantum dots and metal oxide NPs[29,30] have been reported to induce the generation of excess reactive oxygen species (ROS) resulting in modification and damage of cellular proteins, DNA, and lipids, which can lead to cell death.[31] A number of studies have indicated that certain nanomaterials have the potential to initiate spontaneous ROS production based on metal ions and surface characteristics, while other NPs could trigger ROS production only in the presence of certain cell systems.[29,30,32] We chose L929 fibroblasts as target cells to evaluate the cellular compatibility of the biomineralized ZnO NPs, because they were regarded as being very sensitive against ROS. Most studies on the toxicity of ZnO NPs focused on their antibacterial activity; however, the study of their effects on mammalian cells was limited.

Some functionalized NPs, which are coated with binary mixtures of hydrophobic and hydrophilic organic molecules, may be capable of penetrating the cell membrane without overt lipid bilayer disruption/poration.[33] Chiarini[34] and Minoura[35] both reported that SF-coated membrane permitted greater adherence and consequently greater proliferation of fibroblasts in comparison with noncoated membrane. In our work, ZnO NPs with low cytotoxicity to both bacteria and L929 fibroblast cell were fabricated by the process of biomineralization in the template of SF peptide. Obviously, the hydrophilic/hydrophobic chains of SF peptide assembled and coated the surface of ZnO NPs, playing an important role in cellular compatibility. Although the coating layers were not regular on the surface of NPs, SF similar to cell-penetrating peptide[36−38] would be favorable for penetrating cell membranes without disrupting its lipid bilayer. On the other hand, SF peptide coating on ZnO NPs could prevent ROS production based on crystalline surface defects and metal ions.

However, the good biocompatibility of SF peptide could lead to dipping the cell sap into ZnO NPs, showing that SF peptide could be metabolized in cytoplasm to promote cell proliferation (Figures 2 and 3). It was noted that the crystal structure of ZnO NPs did not obviously change inside the cell, and various amino acids in peptide chains on the surface of coated ZnO NPs were correlated with their accumulation inside the cell. Because SF peptide-coated ZnO NPs are kinds of new particles, it is necessary to investigate their toxicological behavior on DNA, and this first report provides such preliminary information in this direction.

## 4. CONCLUSIONS

This paper was concerned with the cellular compatibility of biomineralized ZnO NPs based on prokaryotic and eukaryotic systems. The results showed that ZnO NPs had low toxicity against *E. coli, S. agalactiae, S. aureus,* and L929 cells. Endocytosis of ZnO NPs into the cytoplasm was detected, and the crystal structure of NPs was not destroyed. Meanwhile, mitochondrial cristae, mitochondrial architecture, and all sorts of biomembranes remained

intact. To the best of our knowledge, this was the first report about biomineralized ZnO NPs endowed with excellent compatibility by the process of biomineralization in the template of SF.

## AUTHOR INFORMATION


### Corresponding Author

*Zhongbing Huang: Tel/Fax 86-28-85413003, E-mail zbhuang@iccas.ac.cn, address: No. 3-17, Renmin South Road, Chengdu, Sichuan, 610041, P. R. China. Liang Li: Tel/Fax 86-28-8550 2314, E-mail lilianghx@163.com, address: No. 24, South First Section, First Ring Road, Chengdu, Sichuan, 610065, P. R. China. Baoqing Hao: Tel/Fax 86-28-86714164, E-mail bqhao@mail.sc.cninfo.net, address: No. 16, South Fourth Section, First Ring Road, Chengdu, 610041, P. R. China.


## ACKNOWLEDGMENT


This work has been supported by the National Natural Science Foundation of China (project nos. 60871062 and 50873066). The support of Sichuan Province through a Science Fund for Distinguished Young Scholars of Sichuan Province (08ZQ026-007) and Key Technologies Research and Development Program of Sichuan Province (2008SZ0021 and 2006Z08-001-1) are also acknowledged with gratitude. This work was also supported by the *Research Fund for the Doctoral Program of Higher Education from Ministry of Education of China* (no. 20070610131). We thank Analytical & Testing Center, Sichuan University, for assistance with the microscopy and XRD work.


## REFERENCES


(1) Donaldson, K.; Stone, V.; Clouter, A.; Renwick, L.; MacNee, W. *Occup. Environ. Med.* **2001**, *58*, 211.

(2) OberdÖrster, G.; OberdÖrster, E.; OberdÖrster, J. *Environ. Health Perspect.* **2005**, *113*, 823.

(3) Oberdorster, G.; Stone, V.; Donaldson, K. *Nanotoxicology* **2007**, *1*, 2.

(4) Donaldson, K.; Stone, V.; Tran, C. L.; Kreyling, W.; Borm, P. J. A. *Occup. Environ. Med.* **2004**, *61*, 727.

(5) Berry, C. C.; Charles, S.; Wells, S.; Dalby, M. J.; Curtis, A. S. G. *Int. J. Pharm.* **2004**, *269*, 211.

(6) Berry, C. C.; Wells, S.; Charles, S.; Curtis, A. S. G. *Biomaterials* **2003**, *24*, 4551.

(7) Gupta, A. K.; Gupta, M. *Biomaterials* **2005**, *26*, 1565.

(8) Dunford, R.; Salinaro, A.; Cai, L.; Serpone, N.; Horikoshi, S.; Hidaka, H.; Knowland, J. *Toxicol. Lett.* **1995**, *80*, 61.

(9) Cai, R.; Hashimoto, K.; Itoh, K.; Kubota, Y.; Fujishima, A. *Bull. Chem. Soc. Jpn.* **1991**, *64*, 1268.

(10) Capella, L. S.; Gefé, M. R.; Silva, E. F.; Affonso-Mitidieri, O.; Lopes, A. G.; Rumjanek, V. M.; Capella, M. A. *Arch. Biochem. Biophys.* **2002**, *406*, 65.

(11) Ito, M. *Biomaterials* **1991**, *12*, 41.

(12) Orstavik, D.; Hongslo, J. K. *Biomaterials* **1985**, *6*, 129.

(13) Osamu, Y. *Int. J. Inorg. Mater.* **2001**, *3*, 643.

(14) Stoimenov, P. K.; Klinger, R. L.; Marchin, G. L.; Klabunde, K. J. *Langmuir* **2002**, *18*, 6679.

(15) Huang, Z. B.; Zheng, X.; Yan, D. H.; Yin, G. F.; Liao, X. M.; Kang, Y. Q.; Yao, Y. D.; Huang, D.; Hao, B. Q. *Langmuir* **2008**, *24*, 4140.

(16) Vogelmeier, C.; König, G.; Bencze, K.; Fruhmann, G. *Chest* **1987**, *92*, 946.

(17) Gojova, A.; Guo, B.; Kota, R. S.; Rutledge, J. C.; Kennedy, I. M.; Barakat, A. I. *Environ. Health Perspect.* **2007**, *115*, 403.

(18) Müller, K.; Kulkarni, J.; Motskin, M.; Goode, A.; Winship, P.; Skepper, J.; Ryan, M.; Porter, A. *ACS Nano* **2010**, *4*, 6767.

(19) Colvin, V. L. *Nat. Biotechnol.* **2003**, *21*, 1166.

(20) Hoshino, A.; Fujioka, K.; Oku, T.; Suga, M.; Sasaki, Y. F.; Ohta, T.; Yasuhara, M.; Suzuki, K.; Yamamoto, K. *Nano Lett.* **2004**, *4*, 2163.

(21) Müller, K.; Skepper, J. N.; Posfai, M.; Trivedi, R.; Howarth, S.; Corot, C.; Lancelot, E.; Thompson, P. W.; Brown, A. P.; Gillard, J. H. *Biomaterials* **2007**, *28*, 1629.

(22) Guo, Y.; Wang, H.; He, C.; Qiu, L.; Cao, X. *Langmuir* **2009**, *25*, 4678.

(23) Scheckel, K. G.; Luxton, T. P.; El Badawy, A. M.; Impellitteri, C. A.; Tolaymat, T. M. *Environ. Sci. Technol.* **2010**, *44*, 1307.

(24) Osmond, M. J.; McCall, M. J. *Nanotoxicology* **2010**, *4*, 15.

(25) Yan, D. H.; Yin, G. F.; Huang, Z. B.; Yang, M.; Liao, X. M.; Kang, Y. Q.; Yao, Y. D.; Hao, B. Q.; Han, D. *J. Phys. Chem. B* **2009**, *113*, 6047.

(26) Huang, Z.; Yan, D.; Yang, M.; Liao, X.; Kang, Y.; Yin, G.; Yao, Y.; Hao, B. *J. Colloid Interface Sci.* **2008**, *325*, 356.

(27) Dong, X. X. Methods for testing antibacterial activity of antibacterial materials. In *Antibacterial materials*, Ji, J. H., Shi, W. M., Eds.; Chemical Industry Press: Beijing, 2003; p 293.

(28) Xiao, X. R. *Oral microbiology and applied technology*. Chinese Academy of Medical Sciences and Peking Union Medical College Press: Beijing, 1993; p 160.

(29) Karlsson, H. L.; Cronholm, P.; Gustafsson, J.; Möller, L. *Chem. Res. Toxicol.* **2008**, *21*, 1726.

(30) Lovrić, J.; Cho, S. J.; Winnik, F. M.; Maysinger, D. *Chem. Biol.* **2005**, *12*, 1227.

(31) Xia, T.; Kovochich, M.; Brant, J.; Hotze, M.; Sempf, J.; Oberley, T.; Sioutas, C.; Yeh, J. I.; Wiesner, M. R.; Nel, A. E. *Nano Lett.* **2006**, *6*, 1794.

(32) Green, M.; Howman, E. *Chem. Commun.* **2005**, *1*, 121.

(33) Verma, A.; Uzum, O.; Hu, Y.; Hu, Y.; Han, H.; Watson, N.; Chen, S.; Irvine, D. J.; Stellacci, F. *Nat. Mater.* **2008**, *7*, 588–595.

(34) Chiarini, A.; Petrini, P.; Bozzini, S.; Pra, I. D.; Armato, U. *Biomaterials* **2003**, *24*, 789.

(35) Minoura, N.; Aiba, S.; Higuchi, M.; Gotoh, Y.; Tsukada, M.; Imai, Y. *Biochem. Biophys. Res. Commun.* **1995**, *208*, 511.

(36) Herbig, M. E.; Assi, F.; Textor, M.; Merkle, H. P. *Biochemistry* **2006**, *45*, 3598.

(37) Takeuchi, T.; et al. *Chem. Biol.* **2006**, *1*, 299.

(38) Patel, L. N.; Zaro, J. L.; Shen, W. C. *Pharm. Res.* **2007**, *24*, 1977.